



Epoxidation of alkenes using inorganic polymer of silica zirconia molybdate as catalyst

M. Sharbatdaran ^{a,b}, F. Farzaneh ^{a,*}, M.M. Larijani ^b

^a Department of Chemistry, Alzahra University, Vanak, Tehran, Iran

^b Agricultural, Medical and Industrial Research School, NISTRI, Karaj, Iran



ARTICLE INFO

Article history:

Received 7 March 2013

Received in revised form

29 September 2013

Accepted 10 November 2013

Available online 20 November 2013

Keywords:

Inorganic polymer

Silica zirconia molybdate

Alkenes

Peroxides

Sol-gel synthesis

ABSTRACT

Silica zirconia sulfate was prepared by sol–gel copolymerization of the sulfated zirconium octanoxide and tetraethylorthosilicate (TEOS). Active polymer oxidation catalysts were obtained by introducing sodium molybdate into the polymer by a ligand exchange reaction. The prepared inorganic polymer designated as SZ-Mo was characterized by FT-IR, SEM, XRD, N_2 sorption isotherms, and ICP techniques. It was found that SZ-Mo successfully catalyzes the epoxidation of cyclooctene, cyclohexene, *trans*-stilbene, and norbornene with 22–95% conversion and 60–100% selectivity. The dependence of the SZ-Mo catalytic activity to the amount of adsorbed Mo within the polymer as well as the study of catalyst stability during the course of reactions will be described in this presentation.

© 2013 Elsevier B.V. All rights reserved.

1. Introduction

Epoxidation of alkenes catalyzed by metal complexes is one of the important oxidation reactions in industrial chemistry. Epoxides are important synthetic intermediates for the synthesis of oxygen containing natural or synthetic compounds [1,2]. Many transition metal complexes such as Co, Ti, Mn, V, and Mo have been used as catalyst for epoxidation of cyclic olefins with high selectivity [2]. Molybdenum complexes as the efficient oxyfunctionalization catalysts of alkenes have been the subject of intense research over the last three decades. Different types of molybdenum complexes such as Mo carbonyl derivatives [3,4], molybdenum (VI) aminopyridinium [5], $Mo_2O_6(4,4'$ -ditertbutyl 2,2'-bipyridine)₂ [6], and dioxomolybdenum (VI) complexes of Schiff-bases derivatives [7–10] have been used as catalyst in epoxidation type reactions.

Liquid phase epoxidation is usually performed either in homogeneous or in heterogeneous systems. Due to easier recovery and recycling of the reaction catalysts, many research and developments have been directed on the heterogeneous processes. Different solid supports such as polymers [11,12], silica and silicate layers [13], microporous, mesoporous, and functionalized

mesoporous have been used for immobilization, encapsulation, or incorporation of Mo compounds [14–18].

Recent utilization of inorganic polymer supports such as sulfated silica zirconia materials has attracted much attention in the last years due to their high acidity induced by silica sulfation. These materials are known with the extensive catalytic activities in processes such as isomerization [19], alkylation [20], esterification [21], and those involving oxygenation of hydrocarbons [22].

In this work, inorganic polymer of silica zirconia molybdate was prepared using tetraethylorthosilicate, sulfated zirconia octanoxide, and sodium molybdate. Exploration of factors such as SO_4^{2-}/Zr or Si/Zr and catalytic epoxidation behavior of SZ-Mo with TBHP and H_2O_2 will be discussed.

2. Experimental

2.1. Preparation of the catalysts

2.1.1. Preparation of sulfated silica–zirconia inorganic polymer

The preparation method of silica–zirconia sulphate is almost similar to that of our previously reported for the synthesis of Si-Zr-Mo nanocomposite [23] with minor modification. In a typical procedure, zirconium octanoxide was prepared from zirconium tetra-n-butoxide and 1-octanol by alcohol interchange method. $Zr(Oct)_4 SO_4$ was then prepared by addition of sulfuric acid to different amounts of $Zr(Oct)_4$ solution in order to adjust the SO_4^{2-}/Zr

* Corresponding author. Tel.: +98 21 88258977; fax: +98 21 88041344.

E-mail addresses: faezeh.farzaneh@yahoo.com, Farzaneh@alzahra.ac.ir (F. Farzaneh).

**Scheme 1.** Preparation of SZ1-Mo and SZ2-Mo.

ration as 0.6/1 or 1:1. Zr–Si inorganic polymer designated as SZ1 and SZ2 were prepared with two different molar ratios as follows:

For SZ1: $\text{Zr(Oct)}_2\text{SO}_4$ (4 mmol, 1.80 g), TEOS (40 mmol, 8.87 ml), EtOH (308 mmol, 17.96 ml), H_2O (440 mmol, 7.92 ml), and AcOH (88 mmol, 5.03 ml) and for SZ2: $\text{Zr(Oct)}_2\text{SO}_4$ (4 mmol, 1.80 g), TEOS (4 mmol, 0.89 ml), EtOH (56 mmol, 3.27 ml), H_2O (80 mmol, 1.44 ml), and AcOH (16 mmol, 0.92 ml). Therefore, in a typical procedure, TEOS, ethanol, H_2O , and AcOH were mixed by stirring and $\text{Zr(Oct)}_2\text{SO}_4$ (0.1 M in 1-octanol) was then added under vigorous stirring. The resulting sol was stirred for 3 h. The produced gel was decanted by centrifugation using 3900 r/min for 15 min and then dried at 180 °C for several hours.

2.1.2. Immobilization of Mo on the surface of sulfated silica–zirconia inorganic polymer

MoO_3 (1.5 g, 7.7 mmol) dissolved in NaOH (10 ml, 5 M) was initially titrated with HCl (0.5 M) until pH was adjusted on 7. Sulfated silica–zirconia inorganic polymer (0.5 g) was then added and the mixture heated at reflux for 3 h. Subsequently, the solid product (SZ1-Mo or SZ2-Mo) was decanted by centrifugation, washed with deionized water, and dried at 100 °C.

2.2. Characterization

All chemicals were purchased from Merck chemical company and used without further purification. Infrared spectra were performed (KBr pellets) on a Bruker Tensor 27FT-IR spectrometer. X-ray diffraction (XRD) patterns were recorded on a Philips PW-1800 diffractometer with Cu K α radiation. Chemical analysis of samples was carried out with Varian 150AX inductively coupled plasma optical emission spectrometer (ICP-OES). Electron microscopy was performed on a Vega Tescan, scanning electron microscope (SEM). Surface areas, pore volume, and pore size distributions were obtained from the N_2 isotherms which determined at 77 K using Quantachrome Nova 2200, Version 7.11 Analyzer. The products were analyzed by GC and GC-MS using Agilent 6890 Series, with FID detector, HP-5, 5% phenylmethylsiloxane capillary and Agilent 5973 Network, mass selective detector, HP-5 MS 6989 Network GC system, respectively.

2.3. Catalytic epoxidation

The catalytic reactions were carried out in a round-bottom flask equipped with a magnetic stirrer and condenser. In a typical procedure, the alkene (20 mmol, *trans*-stilbene, 1 mmol), catalyst (50 mg), and CH_3CN (5 ml) were added into the flask. The reaction was started by adding H_2O_2 (20 mmol, 2.04 ml, 30% in H_2O) or TBHP (20 mmol, 2.74 ml, 70% in H_2O). The mixture was heated at reflux for 8 h. The catalyst was filtered and the filtrate was subjected to GC and GC-MS analyses. The Mo, Si, and Zr contents of the recycled catalyst were measured using ICP-OES techniques.

3. Results and discussion

3.1. Characterization of the catalysts

SZ1-Mo and SZ2-Mo were prepared according to the procedure presented in Scheme 1.

The sulfated zirconia was prepared using the reaction between sulfuric acid and Zr(Oct)_4 . Subsequent treatment with a mixture of TEOS, EtOH, AcOH, and distilled H_2O afforded the corresponding

Zr–Si inorganic polymer SZ1 and SZ2. Upon addition of Na_2MoO_4 , SZ1-Mo, and SZ2-Mo were generated presumably via reaction between Zr– SO_4 and MoO_4^{2-} . The weight percentages of Zr, Si, S, and Mo in SZ1, SZ2, SZ1-Mo, and SZ2-Mo were measured using ICP-OES technique in order to calculate the molar ratios of Zr/Si and S/Zr (Tables 1 and 2). The mole ratios of Zr/Si and S/Zr were found to be 0.06 and 1.16 in SZ1 (Table 2) and 0.30 and 1.78 in SZ2 (Table 2), respectively. ICP-OES analysis also showed that weight percents of Mo in SZ1-Mo and SZ2-Mo are 45.42 and 31.31, respectively (Tables 1 and 2). After Mo adsorption, no significant amount of sulfur was detected using ICP-OES technique (Tables 1 and 2). As seen in Table 1, the sulfur moles of SO_4^{2-} anions in SZ-1 and SZ-2 are 0.035 and 0.160, respectively. Moreover, the moles of Mo as MoO_4^{2-} are 0.473 and 0.326, respectively. Based on the results obtained from ICP, EDX, and FT-IR, the MoO_4^{2-} not only have been exchanged with SO_4^{2-} in both SZ-1 and SZ-2, but also some were partly adsorbed on the sample surfaces. Since the surface area of SZ-1 and SZ-2 are 141 and 83 m^2/g respectively, some MoO_4^{2-} may have been exchanged with other anionic species accordingly.

The FT-IR spectrum of $\text{Zr(Oct)}_2\text{SO}_4$ (Fig. 1a) shows vibrations at 500, 610, and 725 cm^{-1} , corresponding to Zr–O bending and stretching vibrations. The bands appearing at 1000–1300, 1300–1400, and 2800–2900 cm^{-1} are attributed to the C–O, CH_3 or CH_2 , and C–H stretching of alkoxy groups, respectively. A broad band displaying at 3400 cm^{-1} is due to the OH stretching associated with alcohol residue present in zirconium alkoxide. Furthermore, the band due to SO_4^{2-} stretching vibrations observed in the range of 900–1200 cm^{-1} is attributed to the symmetric and asymmetric stretching vibrations of S–O bonds present in inorganic chelating bidentate sulfate [20]. The FT-IR spectrum of SZ1 in Fig. 1b displays the bands at 800, 1070, and 1225 cm^{-1} due to the stretching vibrations of Si–O and a band appearing at 520 cm^{-1} belongs to the Si–O bending vibration. The broad bond appearing at 1000–1500 cm^{-1} is probably due to the vibrations of Zr–O–Si group present between ZrO_2 and SiO_2 fragments [21]. As seen in Fig. 1c, the bands displaying at 907 and 960 cm^{-1} corresponding to Mo–O vibration are due to the immobilized Mo on SZ1 polymer [17,24]. Comparison of the FT-IR spectra presented Fig. 1a, b with that shown in Fig. 1c reveals that the MoO_4^{2-} has been exchanged with SO_4^{2-} anions because no vibration due to this group is detected.

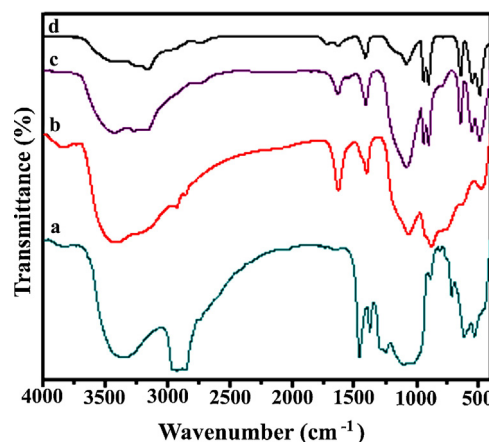


Fig. 1. FT-IR spectra of (a) $\text{Zr(Oct)}_2\text{SO}_4$, (b) SZ1, (c) SZ1-Mo, and (d) SZ1-Mo after used as catalyst.

Table 1

Chemical composition of the prepared materials.

Entry	Sample	Si % (mole)	Zr % (mole)	S % (mole)	Mo % (mol)
1	SZ1	13.77 (0.490)	2.83 (0.031)	1.13 (0.035)	–
2	SZ2	8.50 (0.300)	8.08 (0.089)	5.05 (0.160)	–
3	SZ1-Mo	5.69 (0.203)	1.17 (0.013)	0.000	45.42 (0.473)
4	SZ2-Mo	6.89 (0.250)	7.01 (0.077)	0.000	31.31 (0.326)

Table 2

Physical properties of the prepared materials.

Entry	Sample	(Zr/Si) _{th}	(Zr/Si) _e	(S/Zr) _{th}	(S/Zr) _e	Mo (wt.%)	S _{BET} (m ² /g)	Pore volume (cc/g)	Pore diameter (nm)
1	SZ1	0.10	0.06	0.60	1.16	–	141	0.08	1.19
2	SZ2	1.00	0.30	1.00	1.78	–	83	0.13	1.17
3	SZ1-Mo	0.10	0.06	–	0.00	45.42	37	0.04	2.44
4	SZ2-Mo	1.00	0.31	–	0.00	31.31	79	0.09	1.93

th: theoretical.

e: experimental.

The nitrogen adsorption/desorption isotherms and pore size distribution of SZ1, SZ2, SZ1-Mo, and SZ2-Mo are shown in Fig. 2a–c. Nitrogen adsorption/desorption analyses were performed in order to investigate the textural properties of the resulted compounds. Based on the pore distribution, it is assumed that the isotherm plot is close to type IV and the pores are close to meso species on the basis of IUPAC definition. The calculation of surface area and pore size distribution was obtained based on the BET and BJH methods [25]. The surface area, pore volume, and pore diameter were determined as 141 m²/g, 0.08 cc/g, and 1.19 nm for SZ1 and 83, 0.13, and 1.17 for SZ2, respectively (Table 1). After interchange of SO₄²⁻ with MoO₄²⁻ in SZ1, SZ2 and formation of SZ1-Mo, and SZ2-Mo the surface areas were found to decrease from 141 to 37 and 83 to 79, respectively with concomitant increasing pore volumes and diameters [25,26].

The scanning electron microscopy (SEM) and energy-dispersive X-ray spectroscopy (EDX) results of SZ1, SZ1-Mo, SZ2, and SZ2-Mo

are presented in Fig. 3a–d. The EDX analyses confirm the presence of Si, Zr, and S in the SZ1 and SZ2 and Mo in the SZ1-Mo and SZ2-Mo. The higher Mo content of SZ1-Mo than SZ2-Mo, resulted by comparison of Fig. 3b with d, is also approved by ICP-OES results. The micrographs of SEM reveal that whereas the particle size and morphology of SZ1 and SZ1-Mo differ to some extent, SZ2 and SZ2-Mo have same morphology. Based on the SEM images, SZ1, SZ2, and SZ2-Mo exhibit particles of 20 nm with nearly spherical shape but SZ1-Mo is formed from nanoribbon with preferential growth (Fig. 2b). From the SEM images, one can conclude that polymer with higher amount of Mo may significantly accelerate the formation of crystalline structure together with a better control of the inorganic polymer morphology. The urchin-like-shaped crystals synthesized by microwave heating with Zr and nanorod-shape crystal obtained by the external heating have been already reported [27,28].

Whereas SZ1, SZ2, and SZ2-Mo show no crystalline phase on the basis of the XRD patterns (Fig. 4a–c), the formation of SZ1-Mo in

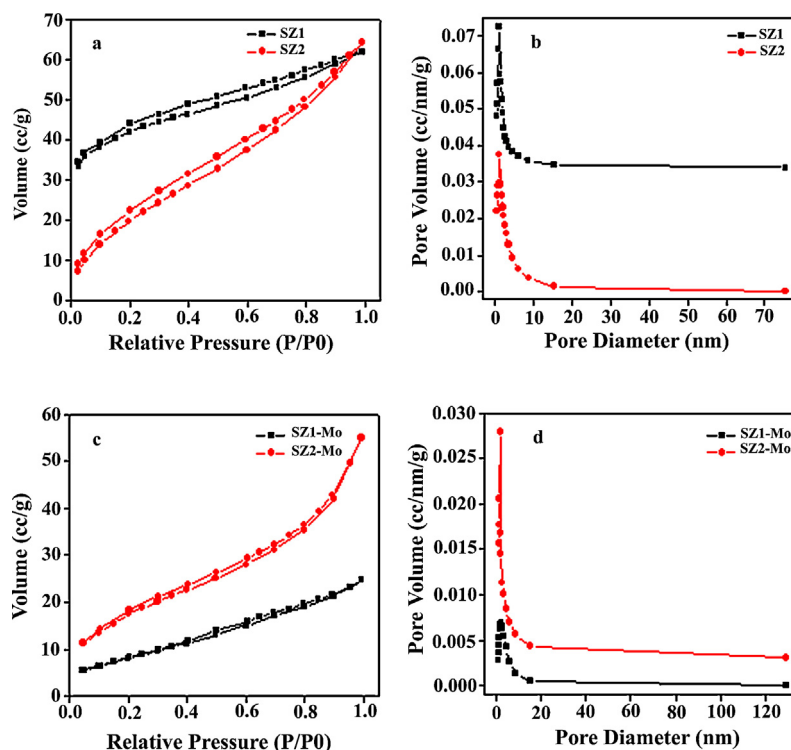


Fig. 2. N₂ adsorption-desorption isotherms and pore size distribution of (a and b) SZ1 and SZ2 and (c and d) SZ1-Mo and SZ2-Mo, respectively.

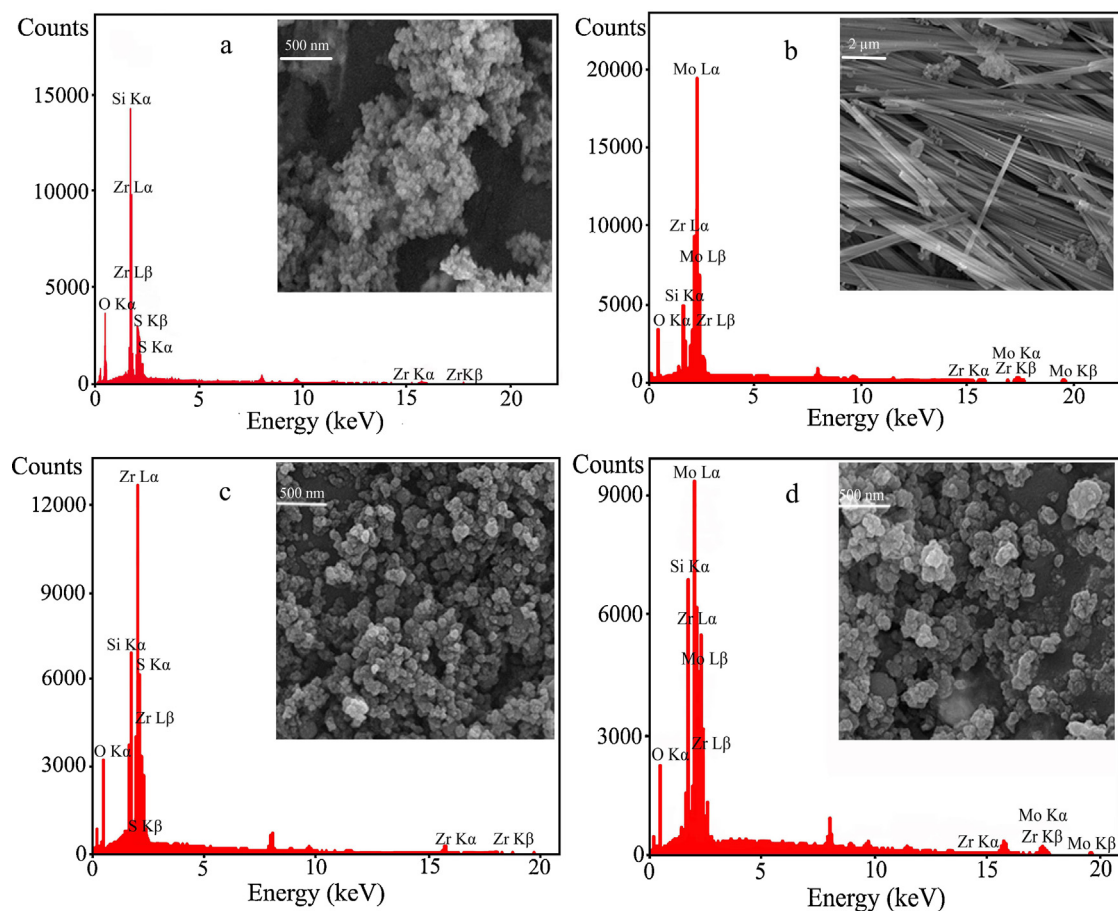


Fig. 3. SEM micrographs and EDX analysis of (a) SZ1, (b) SZ1-Mo, (c) SZ2, and (d) SZ2-Mo.

crystalline phase is evident (Fig. 4d). The crystallinity of SZ1-Mo remains even after using as catalyst is of particular significance.

3.2. Catalytic tests

The SZ1-Mo and SZ2-Mo were used as catalyst for epoxidation of alkenes such as norbornene, *trans*-stilbene, cyclohexene, and cyclooctene. Norbornene was used as the representative substrate for the early exploration of oxidation reactions. In order to study the effect of time on product distribution, reaction times of 0.5, 1, 2, 3, 4, 6, 8, 12, and 24 h were examined in the presence of 50 mg of SZ1-Mo as catalyst and TBHP as oxidant (Fig. 5). Based on the obtained results, the catalytic activity of the prepared catalyst is strongly influenced by the reaction time. As seen, norbornene is oxidized to the corresponding epoxides with 65% conversion and 100% selectivity. Although the conversion increased to 85% by increasing reaction time to 12 h, decrease in selectivity from 100% to 95% with concomitant formation of some norbornyl-*t*-butyl ether was observed.

The effects of the amount of SZ1-Mo shown in Fig. 6 reveal that whereas increasing the amount of catalyst from 20 to 100 mg enhances the conversion from 44 to 81%, decreases in the selectivity occur from 100% to 95%. Based on the optimized conversion and selectivity obtained using 50 mg of catalyst, all the epoxidation reactions were carried out using this amount.

Effect of SZ1-Mo and SZ2-Mo as catalysts on the epoxidation reactions with TBHP is presented in Table 2. Under the same reaction conditions, SZ1-Mo was found to be more reactive in alkene epoxidation in comparison to that of SZ2-Mo. The lower reactivity of SZ2-Mo seems to arise from the lower loading of active

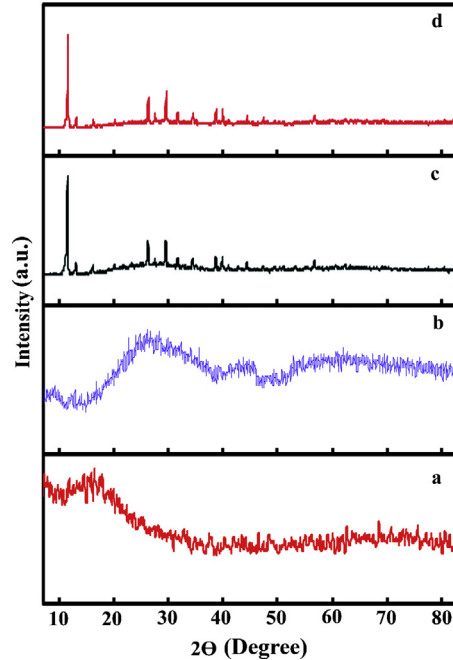


Fig. 4. XRD patterns of (a) SZ2, (b) SZ1, (c) SZ1-Mo and (d) SZ1-Mo after used as catalyst.

Table 3

Oxidation results of alkenes with TBHP in the presence of SZ1-Mo and SZ2-Mo catalysts.

Entry	Alkene	Conversion (%) SZ1-Mo (SZ2-Mo)	Product distribution (%)			TON ^a		
1		85 (66)		94 (92)		6 (8)	- - 71 (81)	
2		80 (38)		61 (26)		26 (53)		13 (21) 67 (47)
3		38 (11)		64 (73)		36 (27)	- - 32 (14)	
4		95 (54)		100 (100)	-	-	3 (3)	

^a The mmol of product to mmol of catalyst, solvent: CH₃CN, alkene (20 mmol), *trans*-stilbene (1 mmol), TBHP (20 mmol), catalyst (0.05 g), time 8 h.

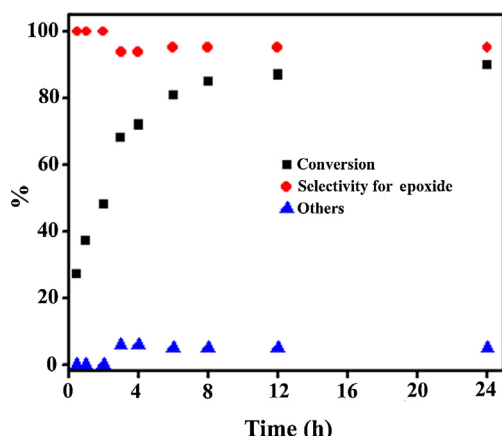


Fig. 5. Kinetic oxidation profiles of norbornene with TBHP over SZ1-Mo catalyst. Reaction conditions: solvent: CH₃CN, norbornene (20 mmol), catalyst (0.05 g), TBHP (20 mmol).

molybdenum sites, perhaps due to the lower BET surface area of the SZ2 precursor.

Quantitative epoxidation of *trans*-stilbene either with SZ1-Mo or with SZ2-Mo is notable (entry 4, Table 3). On the other hand, cyclohexene or cyclooctene undergoes oxidation on both double bond and allylic site, affording epoxide and alcohol or ketone (entries 2 and 3, Table 3). The increase in the ring size of a cyclic olefin decreases the epoxidation rate as reflected in Table 3. The lower activity of cyclooctene may be attributed to the decrease in the ability of cyclooctene for complexation with the catalyst due to the larger steric hindrance [29].

The formation of both double bond and allylic site indicates the involvement of a concerted as well as stepwise oxygen transfer processes from TBHP to the alkene (Scheme 2) [30,31].

The observation of no significant desorption of active catalytic species in the experimental reactions reveals the stability of the

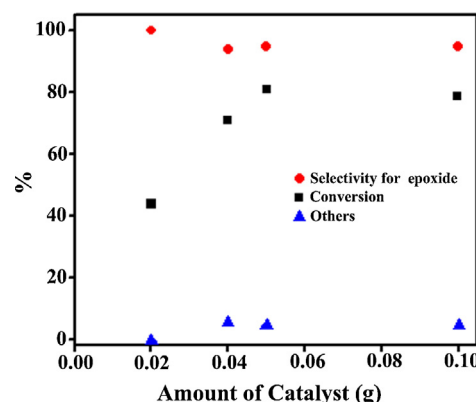
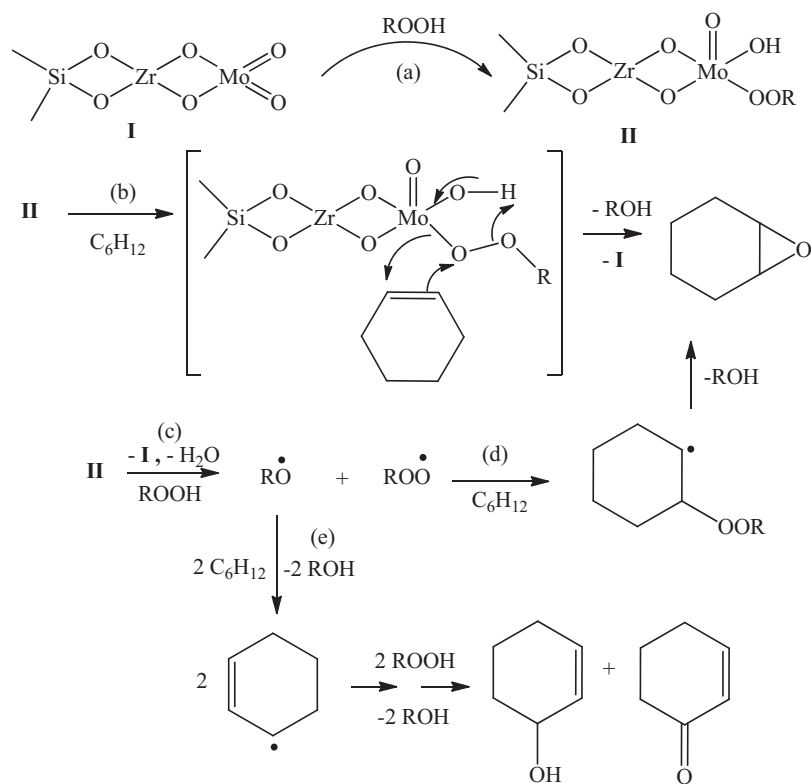


Fig. 6. The effects of catalyst amount on the oxidation of norbornene. Reaction conditions: solvent; CH₃CN, norbornene (20 mmol), TBHP (20 mmol), reaction time: 8 h.

catalytic species under oxidation conditions. The stability of the SZ1-Mo as catalyst was also studied by recycling the recovered catalyst and redetermined the Mo content using ICP techniques. The Mo content of fresh and used catalysts was determined as 45.42 and 45.36%, respectively. ICP determination showed that, no significant amount of Mo content in the filtrate solution. We also found that the catalyst can be recovered and reused at least three times with no significant loss of its catalytic activity. The same determination has been made for SZ2-Mo; the Mo content for fresh and used one was 31.33 and 31.23.

The FT-IR and XRD of SZ1-Mo before and after oxidation reactions were the same (Fig. 1d and Fig. 4d). These results indicate that the SZ1-Mo has survived after using the catalyst in the epoxidation reactions.

The epoxidation results of mentioned olefins with H₂O₂ in acetonitrile catalyzed by SZ1-Mo are given in Table 4. The obtained results indicate that even though the epoxidation selectivity for



Scheme 2. Proposed mechanism for the epoxidation of cyclohexene with SZ1-Mo.

cyclohexene and cyclooctene with H_2O_2 is higher than TBHP, the conversion is lower. The epoxidation of NBD, cyclooctene, and *trans*-stilbene with 100% selectivity is considerable.

Since hydrogenation energies of norbornene, cyclohexene, and cyclooctene are -33.80 , -28.60 , and -22.98 kcal/mole, respectively, 2-norbornyl-*tert*-butyl ether (entry 1, Table 3) may have been generated from addition of *tert*-butanol due to the rather more activity of its double bond [32]. Recall that *tert*-butanol is produced via decomposition of *tert*-butyl hydroperoxide.

A possible mechanism for the inorganic polymer catalyzed oxidation of cyclohexene with H_2O_2 or TBHP is suggested in Scheme 2. Whereas the species responsible for the allylic site oxidation in cyclohexene seems to arise from cleavage of the O–O bond (routes a, c, and e Scheme 2), the epoxidation reaction may have been proceeded either mainly by a concerted reaction of olefin with coordinated ROO radical II (routes a and b, Scheme 2) or partially through a stepwise process (routes a, c, and d Scheme 2). Due to the more efficient epoxidation results indicated in Table 4, implication of H_2O_2 in a concerted reaction with more efficiency seems likely.

Table 4
Oxidation results of alkenes with H_2O_2 in the presence of SZ1-Mo catalyst.

Entry	Alkene	Conversion (%)	Product distribution %	TON ^a
1		51		43
2		94	86 14	78
3		73	100	61
4		22	100	1

^a The mmol of product to mmol of catalyst, solvent: CH_3CN , alkene (20 mmol), *trans*-stilbene (1 mmol), H_2O_2 (20 mmol, 2.04 ml, 30% in H_2O), catalyst (0.05 g), time 8 h.

On the other hand, the preferential participation of TBHP in a step-wise process is anticipated. Such proposal is convincing since the O–O bond in TBHP is 5 kcal/mole weaker in comparison to that of O–O bond present in H₂O₂ [33].

4. Conclusion

Based on the results obtained in this work, it was found that the ratio of Zr/Si and S/Zr plays a crucial role on the particle size, morphology, and surface area of the prepared materials. The novel molybdenum polymers described in this paper exhibit high activity and selectivity in the catalytic epoxidation of olefins. Overall four alkenes were investigated for oxidation either with TBHP or with H₂O₂. The formation of the desired epoxides in higher yields using H₂O₂ was attributed to the stronger peroxide bond of this oxidant. Moreover, the key role of the amount of Mo in catalytic activity was documented by obtaining better results using SZ1-Mo.

Acknowledgement

The authors would appreciate the Alzahra University and Agricultural, Medical and Industrial Research School (AMIRS) for financial support.

References

- [1] K.A. Jorgenson, Chem. Rev. 89 (1989) 431–458.
- [2] T. Punniyamurthy, S. Velusamy, J. Igbal, Chem. Rev. 105 (2005) 2329–2363.
- [3] M. Abrantes, F.A. Almeida Paz, A.A. Valente, C.L. Pereira, S. Gago, A.E. Rodrigues, J. Klinowski, M. Pillinger, I.S. Gonçalves, J. Organomet. Chem. 694 (2009) 1826–1833.
- [4] S. Figueiredo, A.C. Gomes, J.A. Fernandes, F.A. Almeida Paz, A.D. Lopes, J.P. Lourenço, M. Pillinger, I.S. Gonçalves, J. Organomet. Chem. 723 (2013) 56–64.
- [5] J.S. Costa, C.M. Markus, I. Mutikainen, P. Gamez, J. Reedijk, Inorg. Chim. Acta 363 (2010) 2046–2050.
- [6] T.R. Amarante, P. Neves, F.A. Almeida Paz, M. Pillinger, A.A. Valente, I.S. Gonçalves, Inorg. Chem. Commun. 20 (2012) 147–152.
- [7] K. Ambroziak, R. Pelech, E. Milchert, T. Dziembowska, Z. Rozwadowski, J. Mol. Catal. A: Chem. 211 (2004) 9–16.
- [8] A. Rezaeifard, I. Sheikholeslami, N. Monadi, M. Alipour, Polyhedron 29 (2010) 2703–2709.
- [9] N.K. Ngan, Mun Lo D K., Seng D C.H., Wong D R., Polyhedron 30 (2011) 2922–2932.
- [10] X. Lei, N. Chelamalla, Polyhedron 49 (2013) 244–251.
- [11] S. Tangestaninejad, M. Moghadam, V. Mirkhani, I.M. Baltork, M. Torki, C.R. Chim. 14 (2011) 604–610.
- [12] G. Grivani, A. Akherati, Inorg. Chem. Commun. 28 (2013) 90–93.
- [13] G. Wang, L. Feng, R.L. Luck, D.G. Evans, Z. Wang, X. Duan, J. Mol. Catal. A: Chem. 241 (2005) 8–14.
- [14] M. Masteri-Farahani, F. Farzaneh, M. Ghandi, Catal. Commun. 8 (2007) 6–10.
- [15] M. Masteri-Farahani, J. Mol. Catal. A: Chem. 16 (2010) 45–51.
- [16] A.C. Gomes, S.M. Bruno, S. Gago, R.P. Lopes, D.A. Machado, A.P. Carminatti, A.A. Valente, M. Pillinger, I.S. Gonçalves, J. Organomet. Chem. 696 (2011) 3543–3550.
- [17] M. Masteri-Farahani, F. Farzaneh, M. Ghandi, J. Mol. Catal. A: Chem. 243 (2006) 170–175.
- [18] S. Wongkasemjitt, S. Tamuang, W. Tanglumlert, T. Imae, Mater. Chem. Phys. 111 (2009) 301–306.
- [19] R. Akkari, A. Ghorbel, N. Essayem, F. Figueiras, Micropor. Mesopor. Mater. 111 (2008) 62–71.
- [20] M.K. Mishra, B. Tyagi, R.V. Jasra, J. Mol. Catal. A: Chem. 223 (2004) 61–65.
- [21] H. Yang, R. Lua, L. Shena, L. Songa, J. Zhaoa, Z. Wang, L. Wang, Mater. Lett. 57 (2003) 2572–2579.
- [22] G.D. Yadav, J.J. Nair, Micropor. Mesopor. Mater. 33 (1999) 1–48.
- [23] M. Sharbatdaran, L. Jafari Foruzin, F. Farzaneh, M.M. Larjani, C.R. Chim. (2012), <http://dx.doi.org/10.1016/j.crci.2012.10.005>.
- [24] P. Barrett, L.G. Joyner, P.P. Halenda, J. Am. Chem. Soc. 73 (1951) 373–379.
- [25] A.J. Ward, A.A. Pujari, L. Costanzo, A.F. Masters, T. Maschmeyer, Catal. Today 178 (2011) 187–196.
- [26] M. Vasconcellos-Dias, C.D. Nunes, P.D. Vaz, P. Ferreira, P. Brandao, V. Felix, M.J. Calhorda, J. Catal. 256 (2008) 301–311.
- [27] C.V. Ramana, V.V. Atuchin, I.B. Troitskaia, S.A. Gromilov, V.G. Kostrovsky, G.B. Saupe, Solid State Commun. 149 (2009) 6–9.
- [28] M. Osaka, K. Tanaka, Sh. Sekine, Y. Akutsu, T. Suzuki, H. Mimura, J. Nucl. Mater. 427 (2012) 384–388.
- [29] U. Velu, A. Stanislau, G. Virupiah, S.V. Balasubramanian, Chin. J. Catal. 32 (2011) 280–285.
- [30] I.W.C.E. Arends, R.A. Sheldon, Appl. Catal. A: Gen. 212 (2001) 175–187.
- [31] M. Masteri-Farahani, F. Farzaneh, M. Ghandi, J. Mol. Catal. A: Chem. 192 (2003) 103–111.
- [32] F.A. Carey, R.J. Sundberg, Advanced Organic Chemistry, Part A, third ed., Plenum Press, New York, 1990, 383, 716, 110.
- [33] W. Nam, R. Ho, J.S. Valentine, J. Am. Chem. Soc. 113 (1991) 7052–7054.